Steady State Computations Using Summation-by-Parts Operators

Magnus Svärd[*], Ken Mattsson[†], Jan Nordström[‡]

28th March 2003

Abstract

This paper concerns energy stability on curvilinear grids and its impact on steady state calulations. We have done computations for the Euler equations using both high order summation-by-parts block and diagonal norm schemes. The calculations indicate the significance of energy stability in order to obtain convergence to steady state. Furthermore, the difference operators are improved such that faster convergence to steady state are obtained. The numerical experiments also reveal the importance of high quality grids when high order finite difference methods are used.

1 Introduction

Previously, our focus has been on time dependent problems where high order methods are necessary to accurately compute fine structures of the flow. (see [1, 2, 3]) However, those methods need good steady state solutions as initial data which shifted our focus towards computation of such solutions. In this paper we address some key issues relevant to the efficient and accurate computation of steady state solutions by using high order finite difference methods.

There are a variety of methods to speed up convergence but the interest here is properties of the finite difference methods themselves. If a difference

[*]Department of Information Technology, Uppsala University, Uppsala, Sweden.
[†]Department of Information Technology, Uppsala University, Uppsala, Sweden.
[‡]Computational Aerodynamics Department, Aeronautics Division, The Swedish Defence Research Agency, SE-172 90 Stockholm, Sweden.

method have bad properties, convergence to the correct solution will not be possible regardless of any convergence acceleration techniques.

In [4] and [5] summation-by-parts (SBP) operators were developed for Cartesian grids. These operators makes it possible to prove stability using energy estimates. However, in [6] it was shown that stability might be destroyed when a general SBP operator is applied to curvilinear grids and stability is only recovered for a certain class of SBP operators.

Recently, SBP conserving dissipation operators were developed, see [7]. These are of the same order of accuracy as the scheme itself, but can also be used to construct upwind schemes with the proper scaling. In the upwind case, one order of accuracy less is obtained.

Further, in [8], [9], [10] and [11] a theory for imposing boundary conditions using SBP operators with a simultaneous approximation term (SAT) is developed. The SAT boundary procedure can be used both for external and internal boundaries, making the scheme stable for grids composed of blocks. Moreover, this technique gives a straightforward way of efficient parallelization.

The technique mentioned above was used to construct 5th order accurate upwind schemes, which were used to compute steady state solutions to the Euler equations around a NACA0012 airfoil. Both the non-energy stable SBP schemes applied to curvilinenar grids as well as the energy stable schemes are used and compared to each other. To speed up convergence to steady state the difference operators are modified in order to give the smallest spectral radius. Further, local time stepping is used.

The contents of this report are divided as follows: In section 2, the Euler equations are given; section 3 displays the discretization techniques and also an explanation of the parallel implementation; numerical experiments are performed in section 4. In section 5 conclusions are drawn.

2 The Continuous Problem

2.1 Governing Equations

The Euler equations in curvilinear coordinates, $x = x(\xi, \eta)$ and $y = y(\xi, \eta)$, become,

$$\begin{pmatrix} J\rho \\ J\rho u \\ J\rho v \\ J\rho(e + \frac{V^2}{2}) \end{pmatrix}_t + \begin{pmatrix} J\rho(\xi_x u + \xi_y v) \\ J\rho u(\xi_x u + \xi_y v) + J\xi_x p \\ J\rho v(\xi_x u + \xi_y v) + J\xi_y p \\ J(\rho(e + \frac{V^2}{2}) + p)(\xi_x u + \xi_y v) \end{pmatrix}_\xi + \begin{pmatrix} J\rho(\eta_x u + \eta_y v) \\ J\rho u(\eta_x u + \eta_y v) + J\eta_x p \\ J\rho v(\eta_x u + \eta_y v) + J\eta_y p \\ J(\rho(e + \frac{V^2}{2}) + p)(\eta_x u + \eta_y v) \end{pmatrix}_\eta = \begin{pmatrix} 0 \\ 0 \\ 0 \\ 0 \end{pmatrix}$$

where $J = (\xi_x \eta_y - \xi_y \eta_x)^{-1}$; ρ is the density; u, v are the velocity components in the x, y directions respectively; e denotes the internal energy and p the pressure. A complete derivation of these equations is found in [11].

2.2 Lax–Friedrich Flux Splitting

We will formulate the two-dimensional Euler equations using the Lax–Friedrich flux splitting formulation. Consider the 2-D system with m unknowns,

$$\mathbf{u}_t + \mathbf{F}_x + \mathbf{G}_y = 0\,, \quad a \le x \le b\,, \quad c \le y \le d\,, \tag{1}$$

where $\mathbf{u}$ is the solution vector and $\mathbf{F} = \mathbf{A}\,\mathbf{u}$ and $\mathbf{G} = \mathbf{B}\,\mathbf{u}$ are the flux vectors. The matrices $\mathbf{A}$ and $\mathbf{B}$ are the flux Jacobian matrices. We start by splitting the flux vectors into two parts with positive and negative running characteristics respectively. We obtain $\mathbf{F} = \mathbf{A}\,\mathbf{u} = \frac{1}{2}(\mathbf{A} + \alpha\, I_m)\,\mathbf{u} + \frac{1}{2}(\mathbf{A} - \alpha\, I_m)\,\mathbf{u} = \mathbf{A}_+\mathbf{u} + \mathbf{A}_-\mathbf{u}$ and $\mathbf{G} = \mathbf{B}\,\mathbf{u} = \frac{1}{2}(\mathbf{B} + \beta\, I_m)\,\mathbf{u} + \frac{1}{2}(\mathbf{B} - \beta\, I_m)\,\mathbf{u} = \mathbf{B}_+\mathbf{u} + \mathbf{B}_-\mathbf{u}$, where α and β are the largest eigenvalues, in magnitude, to $\mathbf{A}$ and $\mathbf{B}$ respectively and I_m is the $m \times m$ identity matrix. The system (1) can now be written as

$$\mathbf{u}_t + (\mathbf{A}_+\mathbf{u})_x + (\mathbf{A}_-\mathbf{u})_x + (\mathbf{B}_+\mathbf{u})_x + (\mathbf{B}_-\mathbf{u})_y = 0\,. \tag{2}$$

These fluxes will be discretized with upwind and downwind finite difference operators.

3 Computational Procedure

We use numerical schemes with a summation-by-parts (SBP) property for stability reasons. The summation-by-parts properties are the following for the first derivative: Let h denote the spacing between two grid points. Further, let the grid consist of $N+1$ points numbered from 0 to N. Let u denote a grid function and u_x denote its exact derivative projected onto the same grid. Denote by $P^{-1}Q$ an $2m$th order accurate approximation of the first derivative operator,

$$P^{-1}Qu = u_x + [\mathcal{O}(h^{2m-1}), ..., \mathcal{O}(h^{2m-1}), \mathcal{O}(h^{2m}), ...]^T. \tag{3}$$

The operator $P^{-1}Q$ is an SBP operator if i) the matrix P is symmetric and positive definite and defines a norm $\|u\|_P^2 = u^T P u$ and ii) the matrix Q is nearly skew-symmetric and $Q + Q^T = B$, where B is diagonal such that $B = diag[-1, 0, .., 0, 1]$.

3.1 Stability on Curvilinear Grids

The SBP operator above is valid only on equidistant Cartesian grids. Below we will give the conditions for stability on curvilinear grids. The details are found in [6]. Let $\xi(x)$ be a transformation between the x-coordinate and ξ-coordinate and let $x(\xi)$ be the inverse transformation. Consider the advection equation,

$$v_t + v_x = 0, \qquad t \geq 0, \qquad a \leq x \leq b, \text{ or,} \tag{4}$$

$$x_\xi v_t + v_\xi = 0 \qquad t \geq 0, \qquad 0 \leq \xi \leq 1, \tag{5}$$

since $\xi_x^{-1} = x_\xi$ and $\xi(a) = 0$, $\xi(b) = 1$.

The energy rate for equation (4) is obtained by multiplying by v and integrating over x,

$$\frac{d}{dt}||v||^2 = (v(a,t))^2 - (v(b,t))^2. \tag{6}$$

Equation (5) is discretized on $[0, 1]$ with $n + 1$ equidistant points indexed from 0 to n. Let the matrix X_ξ^d be such that, $(X_\xi^d)_{ii} = x_\xi(i\Delta\xi), \quad i = 0...n$, on the diagonal and 0 elsewhere. Let u be the approximate solution to v in each grid point, $u(t) = [u_0(t), u_1(t), ..., u_n(t)]^T$. Then the discretized version of equation (5) becomes,

$$X_\xi^d u_t + P^{-1}Qu = 0, \tag{7}$$

where $P^{-1}Q$ is the difference operator on an equidistant grid previously defined.

In the same manner as in the continuous case, equation (7) is multiplied by $u^T P$ to acquire,

$$u^T P X_\xi^d u_t + u^T Q u = 0.$$

Adding the transpose yields,

$$u^T P X_\xi^d u_t + u_t^T (P X_\xi^d)^T u + u^T (Q + Q^T) u = 0. \tag{9}$$

In general, PX_ξ^d is not a norm since PX_ξ^d is neither positive definite nor symmetric. Thus (9) does not lead to an energy estimate. If PX_ξ^d could be modified to a norm, PX_ξ, equation (9) would be,

$$\frac{d}{dt}(u^T P X_\xi u) + u^T (Q + Q^T) u = 0, \quad or \quad \frac{d}{dt}||u||^2_{PX_\xi} = u_0^2 - u_n^2. \tag{10}$$

i.e. an equation similar to eq (6). Note that if P is diagonal matrix, PX_ξ^d would indeed be a norm since a valid coordinate transformation X_ξ^d is positive definite and diagonal by construction. In fact, this is the only choice to obtain an energy estimate as is shown in [6]. If P is diagonal the boundary can only be closed at half the internal accuracy such that,

$$P^{-1}Qu = u_x + [\mathcal{O}(h^m), ..., \mathcal{O}(h^m), \mathcal{O}(h^{2m}), ...]^T. \tag{11}$$

The global accuracy is then reduced to $m + 1$. However, as will be shown in the next subsection, the loss of efficiency is only minor in the context of upwind operators.

3.2 Artificial Dissipation and Upwind Operators

For nonlinear convection problems it is well known that centered difference schemes require the addition of artificial dissipation to absorb the energy of the unresolved modes. Further, in the previous subsection we claimed that diagonal norms are necessary on nonequidistant grids for stability reasons. If we want to compute a solution with a fifth order method we would have to use an eighth order internal scheme with a fourth order boundary closure. Thus, the internal scheme is unnecessary accurate and wide. However, for stability reasons we add artificial dissipation to cancel terms in the scheme to make it less wide, i.e. we use so called upwinding.

The dissipation operators are of a specific form and the details are given in [7]. The main properties are: $DI_p = P^{-1}R$ with $R = R^T \geq 0$ and DI_p

approximates $d^p\,u/d\,x^p$ in the interior. At the boundary they are constructed to preserve the SBP property and thus they yield stability.

Denote by D_6 the standard difference operator approximating the sixth derivative, i.e. $D_6 = [-1,\ 6,\ -15,\ 20,\ -15,\ 6,\ -1]/h$. Correspondingly $D_8 = [1,\ -8,\ 28,\ -56,\ 70,\ -56,\ 28,\ -8,\ 1]/h$ in the interior. The eighth order internal scheme is $[1/280,\ -4/105,\ 1/5,\ -4/5,\ 0,\ 4/5,\ -1/5,\ 4/105,\ -1/280]$. Then, for the case with an interior accuracy of order eight, we add $DI_8 = D_8/(280 * h)$ and $DI_6 = D_6/(105 * h)$ in the interior and thereby cancel two terms. The interior accuracy is then reduced to fifth order and the operator is only one element wider than the optimal fifth order accurate upwind operator based on block norms. Thus the loss of efficiency using diagonal norm schemes are, for upwind operators, only minor. For the construction the full dissipation operators including the boundary we refer to [7]. We also construct downwind operators in the same manner.

Remark The same technique can be used to construct other upwind operators as well. For example, a third order upwind scheme can be constructed from the third order accurate diagonal norm scheme. Block norm schemes can of course also be used as a basis for the construction of different upwind schemes. As long as the dissipation operators of [7] are used, they will be energy stable.

3.3 The Numerical Scheme

Postponing the boundary treatment we now have the tools to make a semi–discrete discretization of (2). To describe the scheme we will need the following notation,

$$A \otimes B = \begin{bmatrix} a_{0,0}\,B & \cdots & a_{0,q-1}\,B \\ \vdots & & \vdots \\ a_{p-1,0}\,B & \cdots & a_{p-1,q-1}\,B \end{bmatrix}$$

where A is a $p \times q$ matrix and B a $m \times n$ matrix. The $p \times q$ block matrix $A \otimes B$ is called a *Kronecker product*. There are some useful rules for Kronecker products. In this paper we will use $(A \otimes B)(C \otimes D) = (AC) \otimes (BD)$ and $(A \otimes B)^T = A^T \otimes B^T$.

Consider the domain $(a \le x \le b, c \le y \le d)$ with an $N+1 \times M+1$-points equidistant grid. That is,

$$x_i = a + ih_x\,, \qquad i = 0, 1..., N\,, \qquad , h_x = \frac{b-a}{N}, \tag{12}$$

$$y_j = c + jh_y\,, \qquad j = 0, 1..., M\,, \qquad , h_y = \frac{c-d}{M}. \tag{13}$$

The numerical approximation at grid point x_i, y_j is a $1\times m$-vector denoted $\mathbf{v}_{ij}$. We define a discrete solution vector $\mathbf{v}^T = [\mathbf{v}_{11}, \mathbf{v}_{12}, ..., \mathbf{v}_{1M}, \mathbf{v}_{21}, \mathbf{v}_{22}, ..., \mathbf{v}_{NM}]$. The derivative $\mathbf{u}_x$ is approximated with a non-dissipative and pth order accurate finite difference approximation $P_x^{-1}Q_x \otimes I_M \mathbf{v}$, see the description above.

A corresponding semi-discrete approximation of (2) can be written

$$\begin{aligned}\mathbf{v}_t = &- (D_{x+} \otimes I_M \otimes \mathbf{A}_+)\mathbf{v} - (D_{x-} \otimes I_M \otimes \mathbf{A}_-)\mathbf{v} \\ &- (I_N \otimes D_{y+} \otimes \mathbf{B}_+)\mathbf{v} - (I_N \otimes D_{y-} \otimes \mathbf{B}_-)\mathbf{v} \\ = &- (P_x^{-1} Q_x \otimes I_M \otimes \mathbf{A})\mathbf{v} - \alpha\,(P_x^{-1} R_x \otimes I_M \otimes I_m)\mathbf{v} \\ &- (I_N \otimes P_y^{-1} Q_y \otimes \mathbf{B})\mathbf{v} - \beta\,(I_N \otimes P_y^{-1} R_y \otimes I_m)\mathbf{v}.\end{aligned} \tag{14}$$

α and β are the scalings of the artificial dissipation required for the upwind formulation.

3.4 Stable Interface Treatment

As an example of the block interface procedure we will consider,

$$\mathbf{u}_t + \mathbf{A}\mathbf{u}_x + \mathbf{B}\mathbf{u}_y = 0, \qquad -1 \le x \le 0,\ 0 \le y \le 1, \tag{15}$$

$$\mathbf{v}_t + \mathbf{A}\mathbf{v}_x + \mathbf{B}\mathbf{u}_y = 0, \qquad 0 \le x \le 1,\ 0 \le y \le 1. \tag{16}$$

In order to limit the amount of algebra we assume homogeneous boundary conditions. $\mathbf{A}$ and $\mathbf{B}$ are constant symmetric matrices with m rows and columns. The matrices are split according to subsection 2.2. The resulting matrices are denoted A_+, A_- and B_+, B_-.

Discretize the domains with n and l points and in the x direction and k points in the y-direction and denote the $nkm \times 1$, $lkm \times 1$ vectors u and v respectively. Note that the grid lines at the interface match. The difference operators in the x and y direction might be different in the left and right domain and are denoted D^L_{-x}, D^L_{+x}, D^R_{-x}, D^R_{+x}, D^L_{-y}, D^L_{+y}, D^R_{-y} and D^R_{+y}. Further we introduce the following simplifications, $\tilde{I}_L = I_n \otimes I_k \otimes I_m$, $\tilde{I}_R = I_l \otimes I_k \otimes I_m$, $\tilde{\Sigma}_L = I_n \otimes I_k \otimes \Sigma_L$ and $\tilde{\Sigma}_R = I_l \otimes I_k \otimes \Sigma_R$. By using these notations, the semi–discrete system becomes,

$$\begin{aligned}\tilde{I}_L u_t + (D^L_{+x} \otimes I_k \otimes A_+)u + (D^L_{-x} \otimes I_k \otimes \otimes A_-)u & \\ +(I_n \otimes D^L_{+y} \otimes B_+)u + (I_n \otimes D^L_{-y} \otimes B_-)u &= \\ ((P^L_x)^{-1} \otimes I_k \otimes I_m)\tilde{\Sigma}_L(e_N \otimes (u_N - v_0)) + & \\ SAT(x=-1, y=0, y=1), &\end{aligned} \tag{17}$$

$$\begin{aligned}\tilde{I}_R v_t + (D_+^R \otimes I_k \otimes A_+)u + (D_-^R \otimes I_k \otimes A_-)u \\ +(I_l \otimes D_{+y}^R \otimes B_+)v + (I_l \otimes D_{-y}^R \otimes B_-)v &= \\ ((P_x^R)^{-1} \otimes I_k \otimes I_m)\tilde{\Sigma}_R(e_0 \otimes (v_0 - u_N)) + \\ SAT(x=1, y=0, y=1),\end{aligned} \tag{18}$$

where the right hand sides are the SAT penalty terms. Σ_R and Σ_L are unknown $m \times m$ matrices to be determined below by stability. The term $SAT(x=-1, y=0, y=1)$ and $SAT(x=1, y=0, y=1)$ denotes the penalty terms at the outer boundaries. These are scaled to precisely cancel the boundary terms. (See [8, 9, 10, 11] for details.) $e_0 = (1, 0, ..., 0)^T$ and $e_N = (0, ..., 0, 1)^T$ are $l \times 1$ and $n \times 1$ vectors respectively. u_N and v_0 are $km \times 1$ vectors with components corresponding to the interface points. Define the norms $M_L = (P_x^L \otimes P_y^L \otimes I_m)$ and $M_R = (P_x^R \otimes P_y^R \otimes I_m)$. Apply the energy method by multiplying (17) and (18) by $u^T M_L$ and $v^T M_R$ respectively, yielding,

$$\begin{aligned}u^T M_L u_t + u^T(Q_L + R_x^L) \otimes P_y^L \otimes A_+ u + u^T(Q_L - R_x^L) \otimes P_y^L \otimes A_- u + \\ u^T \beta_L (P_x^L \otimes R_y^L \otimes I_m)u = \\ u^T(I_n \otimes P_y^L \otimes \Sigma_L)(e_N \otimes (u_N - v_0))\end{aligned}$$

$$\begin{aligned}v^T M_R v_t + v^T(Q_R + R_x^R) \otimes P_y^R \otimes A_+ v + v^T(Q_R - R_x^R) \otimes P_y^R \otimes A_- v + \\ v^T \beta_R (P_x^R \otimes R_y^R \otimes I_m)v = \\ v^T(I_l \otimes P_y^R \otimes \Sigma_R)(e_0 \otimes (v_0 - u_N)).\end{aligned}$$

Note that the boundary terms at the outer boundaries are cancelled by the SAT terms. Let $\tilde{R}_y^{L,R} = P_x^{L,R} \otimes R_y^{L,R} \otimes I_m$ and $\tilde{R}_x^{L,R} = R_x^{L,R} \otimes P_y^{L,R} \otimes I_m$. Adding the equations to their transposes, using $Q + Q^T = B$ and assuming that $P_y^L = P_y^R = P_y$ yield,

$$\begin{aligned}\frac{d}{dt}(\|u\|_{M_L}^2 + \|v\|_{M_R}^2) = \begin{pmatrix} u_N & v_0 \end{pmatrix} P_y \otimes \mathbf{M} \begin{pmatrix} u_N & v_0 \end{pmatrix}^T \\ -2 \begin{pmatrix} u & v \end{pmatrix} \mathbf{R} \begin{pmatrix} u & v \end{pmatrix}^T.\end{aligned} \tag{19}$$

In (19), $\mathbf{R} = diag(\alpha_L \tilde{R}_x^L + \beta_L \tilde{R}_y^L, \alpha_R \tilde{R}_x^R + \beta_R \tilde{R}_y^R)$ is symmetric and positive semi–definite and

$$\mathbf{M} = \begin{pmatrix} -A + 2\Sigma_L & -\Sigma_L - \Sigma_R \\ -\Sigma_L - \Sigma_R & A + 2\Sigma_R \end{pmatrix}.$$

To obtain stability $\mathbf{M}$ has to be negative semi–definite which is achieved by choosing Σ_L and Σ_R properly.

Since A is a symmetric matrix we can diagonalize it by $X^T A X = \Lambda$, where X is a matrix consisting of the eigenvectors of A. Further, consider penalty parameters Σ_L and Σ_R of the form $X^T \Sigma_L X = \Lambda_L$ and $X^T \Sigma_R X = \Lambda_R$. Denote by λ^i the ith diagonal component of Λ and similarly λ_L^i and λ_R^i for Λ_L and Λ_R. Then we obtain for $i = 1...m$,

$$\lambda_L^i < \frac{\lambda^i}{2}, \tag{20}$$

$$\lambda_R^i = \lambda_L^i - \lambda^i. \tag{21}$$

(The details can be found in [1].) Equation (20) is the stability condition and (21) is recognized as the conservation condition, see for example [9]. With Λ_L and Λ_R determined, inserting $\Sigma_L = X \Lambda_L X^T$ and $\Sigma_R = X \Lambda_R X^T$ in (17) and (18) yields a stable scheme.

Remark It has now been shown how to split the domain of the PDE into two computational domains connected with the SAT method. In two dimensions, the computational blocks have to share the points constituting the internal boundaries at each block interface. This makes the problem particularly easy to parallelize. If each block corresponds to one process on the parallel computer, this process only have to communicate with other processes at the block interfaces, sending and receiving the boundary data at each computational step in time and then computing the solution within the block. With fairly large blocks the amount of communication will be a small part of the total amount of work. If the grid is designed such that each block has approximately the same size, a proper load balance will be achieved.

3.5 Reducing Spectral Radius of $P^{-1}Q$

In order to speed up convergence to steady state it is essential that the spectral radius of the numerical scheme is minimal. In [12], analytical expressions for the first derivative SBP operators of different orders are derived. The free parameters remaining in the operators to close the expressions are in [12] chosen to give the minimal width of the operator near the boundary. However, it is more important to have operators with small spectral radius such that a larger time step may be used. In particular when explicit time stepping is performed. Thus, we have searched the parameter space to find a better choice and indeed it is poosible to severly reduce the spectral radius. In Appendix A in [12] the parameters x_1, x_2 and x_3 for the fifth order diagonal

norm scheme are chosen,

$$\begin{aligned} x_1 &= 1714837/4354560, \\ x_2 &= -1022551/30481920, \\ x_3 &= 6445687/8709120, \end{aligned}$$

to obtain a minimal bandwidth. In our case we choose,

$$\begin{aligned} x_1 &= 0.649 \\ x_2 &= -0.104 \\ x_3 &= 0.755 \end{aligned}$$

and obtain a much smaller spectral radius. For simplicity, we will use the term spectrally optimized to denote the operator with reduced spectral radius though we do not claim that we have found a formal extremum.

In Figure 1 the spectrum of the original fifth order diagonal norm operator is shown as well as the corresonding data for the modified operator. The spectral radii differs by a factor of approximately 9.4. To test the effect of the reduction of the spectral radius we consider the following system of equations,

$$u_t + u_x = 0\,, u(0) = v(0) \tag{22}$$

$$v_t - v_x = 0\,, v(1) = v(1). \tag{23}$$

The system is discretized using the spectrally and non-spectrally optimized operators and a fourth order Runge-Kutta discretization in time. The largest possible quotient $CFL = \Delta t/\Delta x$ was deduced experimentally and found to be $CFL_{opt} = 1.65$ and $CFL_{nonopt} = 0.176$, that is approximately a factor 9.4. This corresponds well to the spectra of the two different discretizations. (See Figure 2.) Further, note that in Figure 2 the eigenvalues are located only in the left halfplane.

As dissipation is added to the operator to make it upwind the spectrum is altered. But it only seems to give a small perturbation of the spectrum and CFL number.

4 Numerical Computations

Next, we consider steady state calculations around NACA0012 at 2 degrees angle of attack and Mach-number (Ma) 0.63. The solution will be calculated using a 2nd and 5th order scheme. The blocking of the grid is shown in Fig.

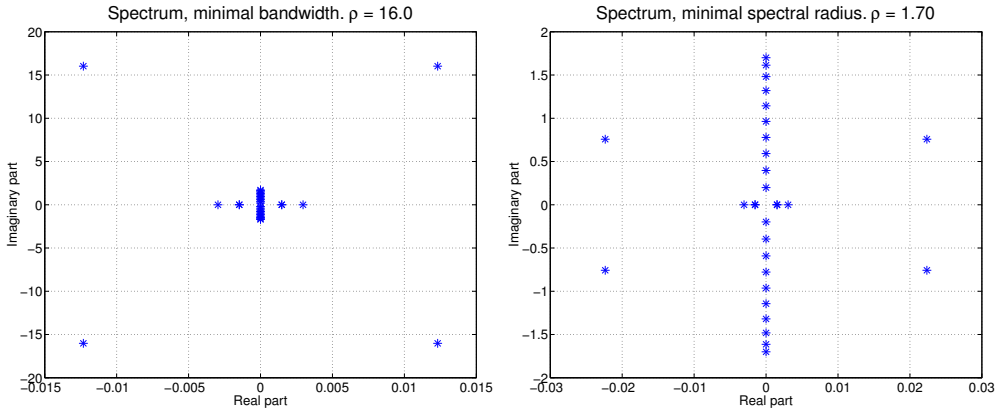

Figure 1: *Left:* Spectrum of original fifth order accurate SBP operator. *Right:* Spectrum of modified fifth order accurate SBP operator.

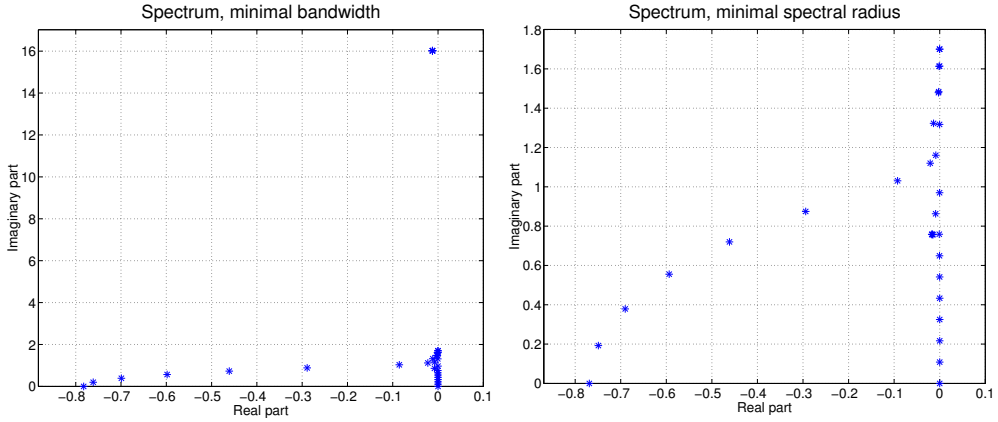

Figure 2: Spectra of the discretized problem (22) and (23). *Left:* Original fifth order accurate SBP operator. *Right:* Modified fifth order accurate SBP operator.

3. The solution is considered to have reached steady state when the residual is less than 10^{-12}.

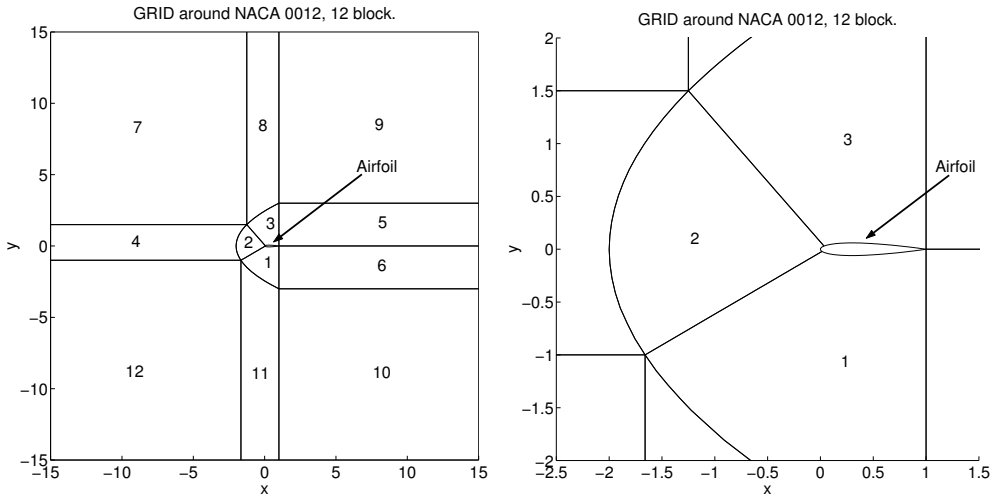

Figure 3: The computational domain around a NACA0012 airfoil divided into 12 blocks. The right subfigure is a close up.

The total amount of grid points and the number of points resolving the airfoil is given in Table 1.

grid	total	airfoil
1	17607	140
2	68402	280
3	269592	560
4	1070372	1120

Table 1: The total number of points in different grids and the resolution of the airfoil.

4.1 Convergence to Steady State.

To investigate the effect of non-energy stable schemes we have computed solutions with the stable fifth order scheme and also with a fifth order block norm scheme (see [12]). The last scheme is not formally stable on the grid since the grid is curvilinear. In Figure 4 the results are shown. It is seen that we do not obtain convergence to steady state with the block norm scheme. In [6] it is shown for a linear equation with zero growth rate that small positive

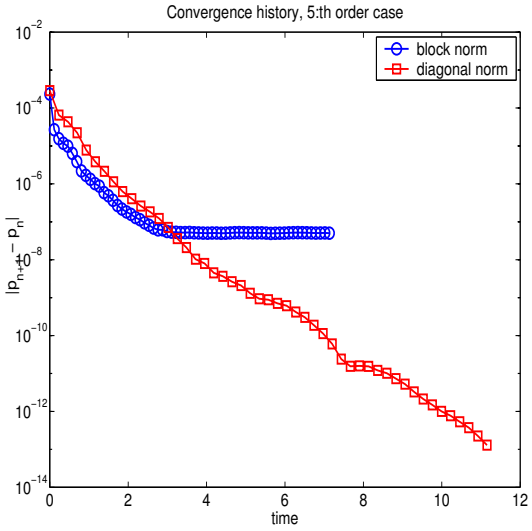

Figure 4: Steady state convergence for fifth order diagonal and block norm scheme.

eigenvalues are obtained when using a block norm scheme. This is probably the reason for not obtaining converegence in this case also. For the diagonal norm schemes no such behavior is observed, see Figure 5. We use a central second order SBP scheme with a fourth order difference (corresponding to a fourth derivative) as artificial viscosity.

Note that even in the non-energy stable scheme case the scheme might be stable. In fact there are several notions of stability. Following the definitions in [13] stability only means boundedness of the growth of the solution. This does not implicate that the time growth of the discrete problem is the same as for the continuous, i.e. regardless of the resolution used, it may be impossible to drive the convergence to steady state arbitrary far. However, if the scheme is strictly stable it means that the time growth converges to the correct growth rate, i.e. for a given residual we can grid refine in space until that demand is fulfilled. Neither of these stability notions are appropriate for steady state calculations since we can in general not afford such grid refinements but want to design the grid only to resolve the expected solution well. Rather, we would like to compute a solution arbitrary close to steady state for a given grid. The energy stable diagonal norm schemes do fulfill this requirement.

Remark Observe that the non-energy stable scheme is stable in the von Neumann sense, i.e. it is stable for the Cauchy problem, even for curvilinear grids. This indicates that the instability is triggered by the boundary

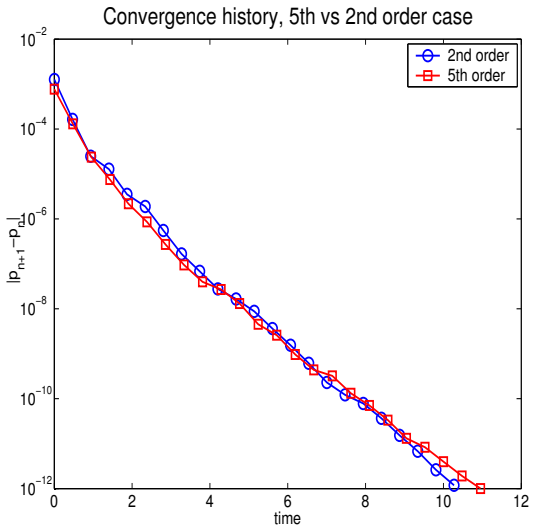

Figure 5: Steady state convergence for fifth and second order accurate diagonal norm schemes.

treatment only.

Furthermore, we consider the same flow case but we compute solutions using the fifth order energy stable non-spectrally and spectrally optimized SBP operators. Also in the airfoil computations the timestep could be increased to the same order of magnitude as for the model equation in subsection 3.5. In this case we gained a factor 9. Of course, the same factor reduces the time to reach steady state. In fact, the timestep can be taken almost as large for the fifth order scheme as for the second order scheme. The difference is approximately 20% which also is the difference in the number of iterations to reach steady state.

4.2 Lift, Drag and Grid Convergence

Next, we turn to steady state computations using only the energy stable spectrally optimized operators on different grids. The same flow case as before is considered. Again we use a reference solution obtained with a central second order SBP scheme and fourth order difference as artificial dissipation. An example of the solution can be seen in Figure 6 where the Mach-number contours computed with the fifth order method on grid 3 is shown.

In order to compare the solutions we compute the lift and drag coeffi-

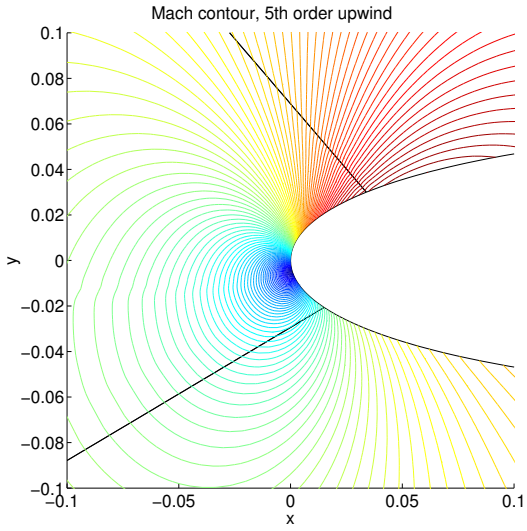

Figure 6: Steady state solution for the fifth order scheme on grid 3. Contour plot of the Mach-number.

cients. The coefficients are defined as follows:

$$c_l = \frac{L}{q_\infty c}, \; c_d = \frac{D}{q_\infty c}, \tag{24}$$

where L, D are the lift and drag forces respectively. q_∞ is the dynamic pressure of the free stream, i.e. $q_\infty = \frac{1}{2}\rho_\infty U_\infty^2$, and c is the cord length. In Table 2 the results are displayed.

$grid$	c_l, $2nd$	c_l, $5th$	c_d, $2nd$	c_d, $5th$
1	0.3277	0.3276	0.00493	0.00362
2	0.3241	0.3246	0.00126	0.00095
3	0.3225	0.3226	0.00046	0.00054
4	0.3217	0.3216	0.00041	0.00042

Table 2: Steady state solutions around NACA0012, $Ma = 0.63$, 2 degrees angle of attack. The lift and drag coefficients for different grids.

Remark In [14] it is shown that for isentropic flow with small disturbances the drag should be zero, that is what is usually called d'Alembert's paradox. This result is obtained via a linearization and hence d'Alembert's paradox only appears in the limit of zero disturbances. In this case we have isentropic flow with a nonzero disturbance and thusly nonzero, but small, drag.

It is seen that the results do not differ much between the methods contrary to what one could expect since the order of accuracy differs. To further

investigate this fact we compute the order of accuracy in the following manner,

$$q = \log\left(\frac{\|u - v^{h1}\|_h}{\|u - v^h 2\|_h}\right) / \log\left(\frac{h1}{h2}\right) \tag{25}$$

where u is the analytic solution and v^{h1}, v^{h2} are corresponding numerical solutions. $\|u - v^{h1}\|_h$ is the l_2-error. In this case no analytic solution is available and we use the 5th order solution on the most well resolved grid as a reference solution. The l_2-errors of the Mach-number are displayed in Table 3.

$grid$	$2nd$	$5th$
1	0.0208	0.0135
2	0.0058	0.0033

Table 3: Steady state solution around NACA0012, $Ma = 0.63$, 2 degrees angle of attack. The l_2-errors of the Mach-number for different grids and order of accuracy.

Remark The l_2-error on grid 3 is not computed since the solution on that grid is too close to the reference solution.

These measures show that the errors are less in fifth order case. However, $q \approx 2$ in both cases. The solution is smooth everywhere except at the trailing edge which causes small disturbances. But still, if the converegence is measured away from the trailing edge where the flow is smooth the same order of accuracy is obtained. This problem will be discussed in the next subsection.

4.3 Open Issues

The question of non-optimal convergence rate of the fifth order method is probably due to a blend of different reasons. At first it is noticed that the grid, obtained with a standard commercial grid generator with an elliptical smoother, yields a bad grid quality index. (That is a measure comparing finite differences of the grid points at different orders of accuracy.) The fifth order method needs three more derivatives of the grid to be smooth in order to yield the correct convergence order compared to a second order method.

Further, the solution of the density shows oscillations in front of the airfoil, see Figure 7. As is seen in Figure 7 the oscillations are reduced as the grid is refined. Similar oscillations are also seen in the second order scheme.

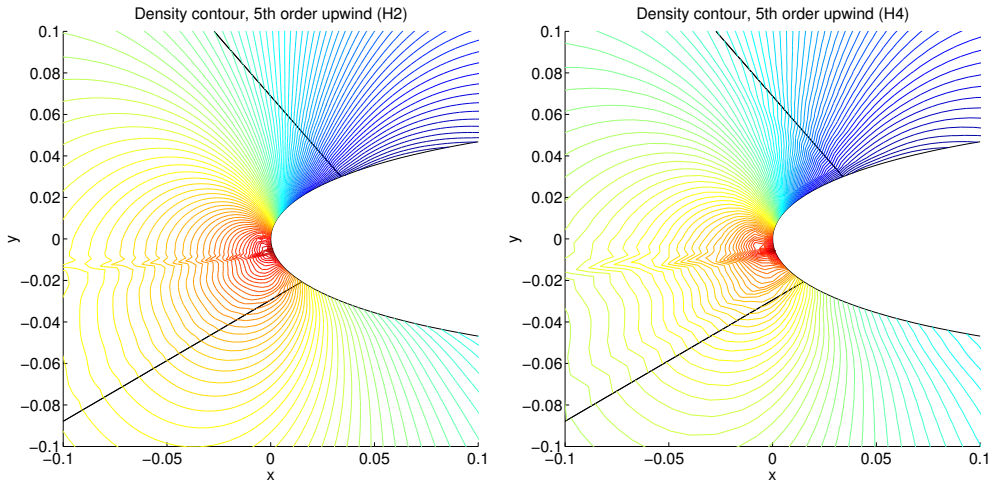

Figure 7: Density contours for the fifth order method on grid 3 (left) and grid 2 (right).

The reason for these oscillations are probably lack of artificial dissipation perpendicular to the symmetry line in the flow solution.

Some preliminary testing supports the above two causes for the reduced convergence rate and a thorough investigation will be done in a future report.

5 Conclusions

We have given numerical evidence that energy stability is important when computing steady state solutions to partial differential equations. On curvilinear grids the SBP block norm schemes are not energy stable as is shown in [6] and accordingly they might yield small positive eigenvalues that destroy convergence to steady state. However, for the diagonal norm scheme no such behavior is observed and in that case stability proofs using the energy method are obtainable.

Furthermore, we have given improvement of the difference operators such that a considerably larger time step may be used. This also contributes to a fast convergence to steady state.

The results at first showed that the fifth order method indeed yield a more accuarate result but the convergence rate was reduced to second order, limiting the gain of such methods. However, numerical evidence indicate that lack of numerical dissipation as well as bad grid quality was the cause of the low convergence rate. It remains to determine what conditions have

to be enforced to recover the correct grid convergence.

References

[1] K. Mattsson, M. Svärd, J. Nordström, and M.H. Carpenter. Accuracy Requirements for Transient Aerodynamics. *AIAA paper 2003-3689*, 2003.

[2] D.W. Zingg. A review of high–order and optimized finite-difference methods for simulating linear wave phenomena. *AIAA paper 97-2088*, 1997.

[3] S. De Rango and D.W. Zingg. Further investigation of a higher-order algorithm for aerodynamic computations. *AIAA paper 2000-0823*, Jan. 2000.

[4] H.-O. Kreiss and G. Scherer. Finite element and finite difference methods for hyperbolic partial differential equations. *Mathematical Aspects of Finite Elements in Partial Differential Equations., Academic Press, Inc.*, 1974.

[5] H.-O. Kreiss and G. Scherer. On the existence of energy estimates for difference approximations for hyperbolic systems. Technical report, Dept. of Scientific Computing, Uppsala University, 1977.

[6] Magnus Svärd. On coordinate transformation for summation-by-parts operators. *Journal of Scientific Computing*, 18, 2003.

[7] Ken Mattsson, Magnus Svärd, and Jan Nordström. Stable artificial dissipation operators for high order finite difference schemes. Technical report 2003-013, Dept. of Information Technology, Uppsala University, 2003.

[8] Mark H. Carpenter, David Gottlieb, and Saul Abarbanel. The stability of numerical boundary treatments for compact high–order finite–difference schemes. *J. Comput. Phys.*, 108(2), 1994.

[9] Mark H. Carpenter, Jan Nordström, and David Gottlieb. A stable and conservative interface treatment of arbitrary spatial accuracy. *J. Comput. Phys.*, 148, 1999.

[10] Jan Nordström and Mark H. Carpenter. Boundary and interface conditions for high order finite difference methods applied to the Euler and Navier–Stokes equations. *J. Comput. Phys.*, 148, 1999.

[11] Jan Nordström and Mark H. Carpenter. High-order finite difference methods, multidimensional linear problems and curvilinear coordinates. *J. Comput. Phys.*, 173, 2001.

[12] Bo Strand. *High–Order difference approximations for hyperbolic initial boundary value problems.* PhD thesis, Uppsala University, Dep. of Scientific Computing, Uppsala Univ., Uppsala, Sweden, 1996.

[13] Bertil Gustafsson, Heinz-Otto Kreiss, and Joseph Oliger. *Time dependent problems and difference methods.* Wiley, New York, 1995.

[14] Jürgen Zierep. *Theoretische Gasdynamik.* G. Braun, Karlsruhe, 1976.